JOURNAL OF COMPUTATIONAL PHYSICS 87, 249–269 (1990)

# Variational Calculation of Electromagnetic Instabilities in Tokamaks

X. GARBET, L. LAURENT, F. MOURGUES, J. P. ROUBIN, AND A. SAMAIN

*Association Euratom-CEA, DRFC, CEN Cadarache, 13108 Saint-Paul-lez-Durance Cedex, France*

Received August 11, 1988; revised February 14, 1989

A variational method is presented in order to determine and study linear microinstabilities in tokamaks. Exploiting the existence of a system of action and angular variables for trapped and circulating particles, a functional, extremum in the turbulent electromagnetic field, is analytically established and implemented in the code TORRID. The coupling of poloidal harmonics due to toroidal effects is investigated within the frame of a WKB formalism whose zeroth order is equivalent to the ballooning analysis. The essential features of the code TORRID are described. Curvature effects on ionic modes profiles and stability thresholds are presented as an example of application. 

## I. INTRODUCTION

Tokamak plasmas are getting closer and closer to thermonuclear conditions. However, they are subject to microscopic instabilities which cause a dramatic reduction of the energy confinement time below its neoclassical value.

Linear theories are available for various instabilities and a lot of work has been done to estimate their nonlinear saturation level, corresponding spectra, and resulting transport across the equilibrium magnetic field. However, the actual mechanism of the microturbulence is still poorly understood. This is largely due to the large number of possible linear instabilities, e.g., electrostatic or not, involving or not involving trapped electrons and ions. The problem of accurately giving the status of all these possibilities in a given plasma is not yet completely solved.

The aim of this paper is to describe a formalism and a derived numerical code taking account of all the possible microinstabilities driven by the diamagnetism in any exact geometry and including all classes of particles. This useful tool predicts the unstable mode structures and parameters (frequency and wave vectors) and also provides the quasilinear transport coefficients. Noncompressional ($\delta B_{\parallel} = 0$), low frequency (smaller than the cyclotronic frequencies) modes are considered, those cases involving most of the instabilities relevant for anomalous transport investigations. Such modes are well described by a perturbed electric potential $\delta U(\mathbf{x}, t)$ and a perturbed potential vector $\delta A(\mathbf{x}, t)$ parallel to the static magnetic field. In the next section, it is shown that a functional extremum for the unstable



0021-9991/90 $3.00

eigenfunctions can be built within the frame of an hamiltonian formalism. A general expression of this functional is derived, taking account of both circulating and trapped particles trajectories in toroidal geometry. As it stands at this level, finding any mode $\delta U$, $\delta A$ is a two-dimensional problem which is hardly tractable numerically. However, the modes in a diamagnetic turbulence exhibit a large scale along the field lines and a small scale in the transverse direction and the problem may be reduced to one dimension through the so-called ballooning formalism. We use that formalism in Section III in the original form under which it has been first introduced [1, 2]: the individual harmonics of each mode determined by a poloidal wave number are localized near the corresponding resonant surface where their parallel wave number vanishes and they exhibit a standard structure about that surface. The computation then reduces to the calculation of this latter structure. The corresponding variational functional is derived, discussed, and compared with previous works [6–9]. It is shown in Section IV that the method is in fact the zeroth order of a WKB analysis taking into account the variations of the structures of the successive poloidal harmonics. This provides criteria for the validity of the approach, which remains numerically tractable. The numerical techniques and the code are described in Section V with some applications to ionic modes.

## II. Physical Features of Electromagnetic Instabilities in Tokamaks

### II.1. *Basic Principle*

We consider a tokamak axisymmetric equilibrium with nested magnetic surfaces labelled by their poloidal magnetic flux $2\pi\Psi$. We define the poloidal angle $\theta$ such that

$$\frac{d\varphi}{d\theta} = q(\Psi) \tag{1}$$

along a field line on a given magnetic surface, $\varphi$ being the usual toroidal angle, and $q(\Psi)$ the safety factor. The equilibrium magnetic field $\mathbf{B}$ may be derived from a potential vector $\mathbf{A}$,

$$\begin{aligned} &\mathbf{B} = \mathbf{rot}\ \mathbf{A} \\ &\mathbf{A} = \phi_T(\Psi)\nabla\theta + \Psi\nabla\varphi, \end{aligned} \tag{2}$$

where $2\Pi\phi_T(\Psi)$ is the flux of the toroidal field through a $\Psi$ magnetic surface and verifies

$$\frac{d\phi_T(\Psi)}{d\Psi} = -q(\Psi). \tag{3}$$

We use the coordinates system $\mathbf{x} = (\Psi, \theta, \varphi)$ whose Jacobian is

$$[\nabla\Psi, \nabla\theta, \nabla\varphi] = -JB = -\frac{B_\varphi}{qR} = -\mathbf{B}\cdot\nabla\theta. \tag{4}$$

Equilibrium density and temperature for each species $s$ are nearly functions of $\Psi$, $n_s(\Psi)$ and $T_s(\Psi)$. We retain the gradients $\partial n_s/\partial\Psi$, $\partial T_s/\partial\Psi$ as the deviation from thermodynamical equilibrium which cause the microinstabilities $\delta E(\mathbf{x}, t)$, $\delta B(\mathbf{x}, t)$. We investigate the modes derived from an electric potential $\delta U(\mathbf{x}, t)$ and a vector potential $\delta A(\mathbf{x}, t)$ directed along the equilibrium field lines,

$$\begin{aligned} &\delta\mathbf{B} = \mathbf{rot}(\delta\mathbf{A}); \qquad \delta\mathbf{A} = \delta A\,\frac{\mathbf{B}}{B} \\ &\delta\mathbf{E} = -\frac{\partial\delta\mathbf{A}}{\partial t} - \nabla\,\delta U, \end{aligned} \tag{5}$$

with an oscillatory time dependence,

$$\begin{aligned} \delta U(\mathbf{x}, t) &= \tilde{U}(\mathbf{x})\exp -i\omega t + cc \\ \delta A(\mathbf{x}, t) &= \tilde{A}(\mathbf{x})\exp -i\omega t + cc. \end{aligned} \tag{6}$$

The fields $\tilde{U}(\mathbf{x})$ and $\tilde{A}(\mathbf{x})$ are $2\pi$-periodic in $\theta$ and $\varphi$. Since the equilibrium is axisymmetric in $\varphi$, a single $\varphi$ Fourier harmonic can be kept so that

$$\begin{aligned} \tilde{U}(\mathbf{x}) &= \sum_l U_l(\Psi - \Psi_l)\exp i(l\theta + m\varphi) \\ \tilde{A}(\mathbf{x}) &= \sum_l A_l(\Psi - \Psi_l)\exp i(l\theta + m\varphi), \end{aligned} \tag{7}$$

where for each $\theta$-harmonic $l$, a $\Psi$ structure around the resonant surface $\Psi = \Psi_l(q(\Psi_l) = -l/m)$ has been introduced. In the computations, those structures in fact will be specified by the Fourier transforms

$$(U_l(\Psi - \Psi_l), A_l(\Psi - \Psi_l)) = \int_{-\infty}^{+\infty} \frac{dK}{2\pi}\,(U_l(K), A_l(K))\exp iK(\Psi - \Psi_l). \tag{8}$$

By perturbing the particle trajectories of each species $s$, the fields $\tilde{U}(\mathbf{x})$, $\tilde{A}(\mathbf{x})$ induce a current density $\tilde{j}_s(\mathbf{x})$ and a charge density $\tilde{\rho}_s(\mathbf{x})$ depending on $\tilde{U}(\mathbf{x})$, $\tilde{A}(\mathbf{x})$ through a linear operator. The Maxwell equations, reduced here to the Ampère equation along the field lines and the electroneutrality constraint, can be written in a synthetic variational form, whose functional, bilinear in $\tilde{U}^*$, $\tilde{A}^*$ and in $\tilde{U}$, $\tilde{A}$ is

$$\mathscr{L}(\tilde{U}^*, \tilde{A}^*, \tilde{U}, \tilde{A}) = = -\frac{1}{\mu_0}\int d_3\mathbf{x}\,|\nabla\mathbf{x}\tilde{A}|^2 + \sum_s \mathscr{L}_s, \tag{9}$$

where for each species $s$:

$$\mathscr{L}_s(\tilde{U}^*, \tilde{A}^*, \tilde{U}, \tilde{A}) = \int d_3\mathbf{x}(\tilde{j}_s\tilde{A}^* - \tilde{\rho}_s\tilde{U}^*).$$

The $\mathscr{L}_s$ functionals are linear in $\tilde{U}$, $\tilde{A}$ through $\tilde{\rho}_s$, $\tilde{j}_s$. The field equations for $\tilde{U}$, $\tilde{A}$ are equivalent to state that the functional is an extremum with respect to $\tilde{U}^*$ and $\tilde{A}^*$. For $\omega$ real, the power transferred by the RF field to the species $s$ is equal to $2\omega$ Im $\mathscr{L}_s$. We will calculate $\mathscr{L}_s$ under the form

$$\mathscr{L}_s = \int d_3\mathbf{x} \frac{n_s e_s^2}{T_s} \tilde{U}(\mathbf{x})\, \tilde{U}^*(\mathbf{x}) + \mathscr{L}_{sres}. \tag{10}$$

The procedure is convenient because a standard expression for the functional $\mathscr{L}_{sres}$ is available in a resonant form (Eq. (18)), when the unperturbed particle trajectories are integrable.

II.2. *Unperturbed Trajectories*

Since the tokamak confinement properties are basically related to the integrability of the trajectories in the equilibrium field, it is fruitful to introduce a Hamiltonian formalism so as to compute the plasma responses $\tilde{n}_s$ and $\tilde{j}_s$. For given adiabatic magnetic moment $\mu(\mathbf{x}, \mathbf{p}) = m_s v_\perp^2/2B$, energy $H(\mathbf{x}, \mathbf{p}) = \frac{1}{2}m_s v_\parallel^2 + \mu B$ and momentum around the major axis $M(\mathbf{x}, \mathbf{p}) = e_s\Psi + m_s v_\varphi R$ (the three basic constants of the motion), the position of a particle in the phase space $(\mathbf{x}, \mathbf{p})$ depends periodically on three angular variables $\phi_1(\mathbf{x}, \mathbf{p})$, $\phi_2(\mathbf{x}, \mathbf{p})$, $\phi_3(\mathbf{x}, \mathbf{p})$ varying linearly in time along any unperturbed trajectory. More precisely, the cyclotronic motion depends on a gyrophrase $\phi_1 = \omega_1(H, \mu, M)\, t + \phi_{10}$ ($\omega_1$ is the time average value of the cyclotronic frequency $\omega_{cs} = -e_s B/m_s$) while the guiding center motion ($\Psi_G$, $\theta_G$, $\varphi_G$) is described by two slowly varying phases $\phi_2 = \omega_2(H, \mu, M)\, t + \phi_{20}$ and $\phi_3 = \omega_3(H, \mu, M)\, t + \phi_{30}$ ($\phi_{10}$, $\phi_{20}$, $\phi_{30}$ are initialization constants). The following equations are available from preliminary computations, either for the case where the parallel velocity $v_\parallel = \pm\sqrt{2(H - \mu B)/m_s}$ cancels during the motion and the particle is trapped or for the case where $v_\parallel$ does not vanish and the particle circulates around the major axis. Instead of the moment $M$, a flux $\bar{\Psi}(\mu, H, M)$ will be used as the third constant of the motion ($\bar{\Psi}$ can be, for instance, the time averaged value of $\Psi_G$).

(i) *Circulating particles.* The variables $\phi_2$, $\phi_3$ represent the phases of the guiding center motion around the magnetic axis and the major axis respectively and for given $H$, $\mu$, $\bar{\Psi}$,

$$\begin{aligned} \theta_G &= \bar{\varepsilon}\phi_2 + \hat{\theta}(\phi_2) \\ \varphi_G &= \phi_3 + q(\bar{\Psi})\, \hat{\theta}(\phi_2) + \hat{\varphi}(\phi_2) \\ \Psi_G &= \bar{\Psi} + \hat{\Psi}(\phi_2), \end{aligned} \tag{11}$$

where $\bar{\varepsilon}=1$ and $\hat{\theta}$, $\hat{\varphi}$, and $\hat{\Psi}$ are $2\pi$ periodic functions of $\phi_2$ representing the $v_\parallel$ modulation due to the inhomogeneity of $B$ and the curvature drift effects. The frequency $\omega_2=d\phi_2/dt$ and the function $\hat{\theta}$ are needed in what follows at zeroth order only with respect to the ion Larmor radius, namely,

$$\omega_2=1\Big/\int_0^{2\pi}\frac{d\theta}{2\pi J v_\parallel}$$
$$\hat{\theta}=\int_0^{\phi_2}d\phi_2\left(\frac{Jv_\parallel}{\omega_2}-\bar{\varepsilon}\right), \tag{12}$$

where the integrand must be considered as functions of $\theta$ or $\phi_2$ along a trajectory specified by $\mu$, $H$, $\bar{\Psi}$, and $\mathrm{sign}(v_\parallel)$. At first order in Larmor radius, we then have

$$\omega_3=\bar{\varepsilon}q(\bar{\Psi})\,\omega_2+\omega_d$$
$$\omega_d=\int_0^{2\pi}\frac{d\phi_2}{2\pi}\left\{\left(\nabla\varphi-\frac{dq}{d\Psi}\hat{\theta}\,\nabla\Psi-q\,\nabla\theta\right)\cdot v_g+\bar{\varepsilon}\frac{dq}{d\Psi}\omega_2\hat{\Psi}\right\}, \tag{13}$$

where $\mathbf{v}_\mathbf{g}=(\mathbf{B}/e_s B^2)\,\mathbf{x}(m_s v_\parallel^2(\mathbf{1}/\mathbf{R})+\mu\,\nabla B)$ is the drift velocity due to the field curvature. Moreover,

$$\hat{\varphi}=\frac{dq}{d\Psi}\left(\hat{\theta}\hat{\Psi}+\bar{\varepsilon}\int_0^{\phi_2}d\phi_2\,\hat{\Psi}\right)$$
$$+\int_0^{\phi_2}\frac{d\phi_2}{\omega_2}\left\{\left(\nabla\varphi-\frac{dq}{d\Psi}\hat{\theta}\,\nabla\Psi-q\,\nabla\theta\right)\cdot\mathbf{v}_\mathbf{g}-\omega_d\right\} \tag{14}$$
$$\hat{\Psi}=\int^{\phi_2}\frac{d\phi_2}{\omega_2}(\nabla\Psi\cdot\mathbf{v}_\mathbf{g}).$$

(ii) *Trapped particles.* The variables $\phi_2$ and $\phi_3$ are now the phases of the bounce motion and the precession motion around the major axis. Equations (11), (12) apply with $\bar{\varepsilon}=0$ rather than $\bar{\varepsilon}=1$. The frequency $\omega_2=d\phi_2/dt$ is the bounce frequency given by

$$\omega_2=1\Big/\int_{-\theta_0}^{\theta_0}\frac{d\theta}{\pi\,Jv_\parallel}, \tag{15}$$

where $[-\theta_0,\,\theta_0]$ is the bouncing $\theta$ interval depending on $\mu$, $H$, $\bar{\Psi}$. The formulas (13), (14) remain correct with $\bar{\varepsilon}=0$.

II.3. *Expression of the Functional $\mathscr{L}_{sres}$*

The coordinates system ($\mu$, $H$, $\bar{\Psi}$, $\phi_1$, $\phi_2$, $\phi_3$) allows to obtain a very simple expression of the functional within the frame of an Hamiltonian formalism. The Hamiltonian perturbation associated with the fields $\tilde{U}(\mathbf{x})$, $\tilde{A}(\mathbf{x})$,

$$\tilde{h}(\mathbf{x},\mathbf{p})=e_s(\tilde{U}(\mathbf{x})-v_\parallel(\mathbf{x},\mathbf{p})\,\tilde{A}(\mathbf{x})) \tag{16}$$

may be expanded as a Fourier series in $\phi_1, \phi_2, \phi_3$,

$$\tilde{h}(\mathbf{x}, \mathbf{p}) = \sum_{n_1, n_2} h_{n_1, n_2}(\mu, H, \bar{\Psi}) \exp\{i(n_1\phi_1 + n_2\phi_2 + m\phi_3)\}. \tag{17}$$

Solving the Vlasov equation within that frame, the functional $\mathscr{L}_{sres}$ for a particle species $s$ is found to be [4, 5]

$$\mathscr{L}_{sres} = -\sum_{n_1, n_2} \int d_3\mathbf{x}\, d_3\mathbf{p} \frac{F_s}{T_s} \frac{\omega - \omega_s^*}{\omega - n_1\omega_1 - n_2\omega_2 - m\omega_3 + i\varepsilon} |h_{n_1, n_2}|^2, \tag{18}$$

where

$$F_s(H, \bar{\Psi}) = \frac{n_s(\bar{\Psi})}{(2\pi m_s T_s(\bar{\Psi}))^{3/2}} \exp -\frac{H}{T_s(\bar{\Psi})}$$

is the equilibrium distribution function on the surface $\Psi = \bar{\Psi}$ and

$$\omega_s^* = m\frac{T_s}{e_s} \frac{\partial \operatorname{Log} F_s(H, \bar{\Psi})}{\partial \bar{\Psi}} \tag{19}$$

is the $H$ dependent diamagnetic frequency measuring the radial gradients.

For the low frequency turbulence considered, $\omega \sim \omega_s^* \ll \omega_1 \sim \omega_{cs}$, only the components $h_{n_1, n_2}$ for which $n_1 = 0$ play a role. They are obtained by averaging $\tilde{h}(\mathbf{x}, \mathbf{p})$ over the cyclotron motion, an operation which, for given slow variables $\mu$, $H$, $\Psi_G$, $\theta_G$, $\varphi_G$, is equivalent to the integration $\int_0^{2\pi} (d\phi_1/2\pi)\, \tilde{h}(\mathbf{x}, \mathbf{p})$. Starting from the expressions (7) and (8) and performing this averaging, it finally becomes

$$h_{0, n_2} = \sum_l \int_{-\infty}^{+\infty} \frac{dK}{2\pi} \int_0^{2\pi} \frac{d\phi_2}{2\pi} J_0(a_l(K, \phi_2)) \times e_s(U_l(K) - v_\parallel(\phi_2)\, A_l(K)) \exp\{i(B_l(K, \phi_2) - n_2\phi_2)\}, \tag{20}$$

where the arguments of the Bessel function $J_0$,

$$a_l(K, \phi_2) = \left|\frac{\mathbf{B}}{B} \mathbf{x} \nabla(K\Psi + l\theta + m\varphi)\right| \left(\frac{2\mu B}{m_s \omega_{cs}^2}\right)^{1/2} \tag{21}$$

and

$$v_\parallel(\phi_2) = \pm \sqrt{2(H - \mu B)/m_s} \tag{22}$$

are calculated for $\mu$, $H$ given at $\Psi = \bar{\Psi}$ and $\theta = \bar{\varepsilon}\phi_2 + \hat{\theta}(\phi_2)$; $\bar{\varepsilon} = 1$ or 0 in the circulating or trapped domain. The function $B_l$ represents the phase perturbations experienced by a particle during its motion,

$$B_l(K, \phi_2) = l\,\bar{\varepsilon}\,\phi_2 + K(\bar{\Psi} - \Psi_l) + (l + mq(\bar{\Psi}))\,\hat{\theta}(\phi_2) + m\hat{\varphi}(\theta_2) + K\hat{\Psi}(\phi_2). \tag{23}$$

The formula (20) included in the $\mathscr{L}_{sres}$ expression (18) for each species allows us to complete the calculation of the functional $\mathscr{L}$ (9), (10).

In a cylindrical equilibrium where $\hat{\theta} = \hat{\varphi} = \hat{\Psi} = 0$, there exists a single relevant number $n_2 = l$ for a given $l$ component $U_l(\Psi - \Psi_l)$, $A_l(\Psi - \Psi_l)$ of the field $\tilde{U}(\mathbf{x})$, $\tilde{A}(\mathbf{x})$. The toroidicity introduces $\phi_2$ dependent functions $a_l$, $v_\parallel$, $B_l$ and therefore additional relevant numbers $n_2 = l \pm 1$, $l \pm 2$, ..., in the circulating domain. In the trapped domain, the relevant $n_2 = 0$, $\pm 1$, $\pm 2$, ..., represent the harmonics of the bounce motion involved in the response of the particles. Conversely, a given $n_2$ involves several components $U_l$, $A_l$ which are then coupled in the functional $\mathscr{L}$. The latter may be formally written

$$\mathscr{L} = \sum_{l,l'} \mathscr{L}_{l,l'}(U_l^*, A_l^*, U_{l'}, A_{l'}). \tag{24}$$

In the absence of toroidal effects, the functionals $\mathscr{L}_{l,l'}$ vanish for noncancelling $l' - l$ differences. Hence, $\mathscr{L}$ can be extremized for each mode $l$ independently of the others. It is essential that those modes are found localized by magnetic shear near the resonant surface $\Psi = \Psi_l$, where $l + mq(\Psi_l) = 0$. This allows us to take into account the coupling between $l$ and $l'$ components introduced by the toroidal effects by using a WKB scheme along $l$ of the successive structures $U_l(\Psi - \Psi_l)$, $A_l(\Psi - \Psi_l)$, equivalent to the so-called ballooning approximation, which is detailed in the following sections.

## III. The Standard Structures $U_l(\Psi - \Psi_l)$, $A_l(\Psi - \Psi_l)$ or Their Fourier Transforms $U_l(K)$, $A_l(K)$

### III.1. *l-translating Invariance*

The coupling terms $\mathscr{L}_{l,l'}$ in (24) reflect the variation $\exp\{i(l - l')\theta\}$ of the equilibrium configuration and are effective for a few values of $|l - l'|$. At large $l$, $m$, the successive surfaces $\Psi_l$, $\Psi_{l+1}$, ..., are close together. If each $\theta$ harmonic $U_l(\Psi - \Psi_l)$, $A_l(\Psi - \Psi_l)$ is localized near the corresponding resonant surface $\Psi = \Psi_l$, the functionals $\mathscr{L}_{l,l'}$ which reflect the properties of the plasma in the neighbouring of the surface $\Psi_l$, weakly depends on $l$, at given $l' - l$. In this section, we exploit that situation at lowest order by assuming that the $\Psi$-distance

$$d = -\frac{1}{m \left.\dfrac{\partial q}{\partial \Psi}\right|_{\Psi = \Psi_l}}$$

between two adjacent resonant surfaces does not depend on $l$ and the functionals $\mathscr{L}_{l,l'}$ depend only on $l' - l$.

The functional $\mathscr{L}(\tilde{U}^*, \tilde{A}^*, \tilde{U}, \tilde{A})$ is then invariant under the transformation $\tilde{U}$, $\tilde{A} \to \tilde{U}'$, $\tilde{A}' = \mathscr{C}(\tilde{U}, \tilde{A})$ defined by

$$(U_l'(\Psi - \Psi_l), A_l'(\Psi - \Psi_l)) = (U_{l+1}(\Psi - \Psi_{l+1}), A_{l+1}(\Psi - \Psi_{l+1})). \tag{25}$$

This means that the operator $\mathscr{K}(U, A) = \partial \mathscr{L}(\tilde{U}^*, \tilde{A}^*, \tilde{U}, \tilde{A})/\partial(\tilde{U}^*, \tilde{A}^*)$ commutes with $\mathscr{C}$. These two operators therefore exhibit a common set of eigenfunctions, i.e., a physical eigenmode satisfying the equation

$$\mathscr{K}(\tilde{U}, \tilde{A}) = 0 \tag{26}$$

may be written as an eigenvector of $\mathscr{C}$ associated with the eigenvalue $\exp(il\delta)$,

$$(U_l(\Psi - \Psi_l), A_l(\Psi - \Psi_l)) = (U(\Psi - \Psi_l), A(\Psi - \Psi_l)) \exp il\delta, \tag{27}$$

where $\delta$ is a real constant and $U(X)$, $A(X)$ are standard functions localized near $X = 0$ which are handled in computations by their Fourier transforms,

$$(U(X), A(X)) = \int_{-\infty}^{+\infty} \frac{dK}{2\pi} (U(K), A(K)) \exp(iKX). \tag{28}$$

This situation of an infinite sequence of identical modes localized on each resonant surface is equivalent to the usual ballooning approximation (Appendix 1).

III.2. *Calculation of the Functionals $\mathscr{L}_{sres}$*

Choosing a reference poloidal number $l_0$ associated with $\Psi_{l_0}(q(\Psi_{l_0}) = -l_0/m)$ we obtain by substitution of (28) in (20) for each set of constant of motion $\mu$, $H$, and $\bar{\Psi}$,

$$\begin{aligned} |h_{0,n_2}|^2 = \sum_{l,l'} \iint_0^{2\pi} \frac{d\phi_2}{2\pi} \frac{d\phi_2'}{2\pi} \iint_{-\infty}^{+\infty} \frac{dK}{2\pi} \frac{dK'}{2\pi} \\ \times J_0(a_l(K, \phi_2))\, h(K, \phi_2)\, J_0(a_l(K', \phi_2'))\, h^*(K', \phi_2') \\ \times \exp\{i(B_l(K, \phi_2) - B_{l'}(K', \phi_2') + (l - l')\,\delta - n_2(\phi_2 - \phi_2'))\}, \end{aligned} \tag{29}$$

where $h(K, \phi_2) = e_s(U(K) - v_\parallel(\phi_2)\, A(K))$.

Noting that

$$B_l(K, \phi_2) = B_{l_0}(K, \phi_2) + (l - l_0)(\bar{\varepsilon}\phi_2 + \hat{\theta}(\phi_2) - Kd) \tag{30}$$

and using the identity

$$\sum_l \exp\{i(l - l_0)(\theta + \delta - Kd)\} = \frac{2\pi}{|d|} \sum_p \delta\left(K - \frac{(\theta + \delta + 2p\pi)}{d}\right) \tag{31}$$

to perform the summations in $l$, $l'$, then integrating the $\delta$ functions over $K$ and $K'$, and finally taking into account that the sums over $p$ allow to transform the $\phi_2$, $\phi_2'$ integrals over $[0, 2\pi]$ in integrals over $[-\infty, +\infty]$, one may transform Eq. (29) into

$$|h_{0,n_2}|^2 = \iint_{-\infty}^{+\infty} \frac{d\phi_2}{2\pi}\frac{d\phi_2'}{2\pi}\frac{1}{d^2} J_0(a(\phi_2))\, h(\phi_2)\, J_0(a(\phi_2'))\, h^*(\phi_2')$$
$$\times \exp\left\{ i\left( \Lambda(\phi_2) - \Lambda(\phi_2') + \left( l_0 + \frac{\bar{\Psi} - \Psi_{l_0}}{d} \right) (\mathscr{E}(\phi_2) - \mathscr{E}(\phi_2')) \right.\right.$$
$$\left.\left. - n_2(\phi_2 - \phi_2') \right) \right\}, \tag{32}$$

where

$\mathscr{E}(\phi_2) = \phi_2$ in the circulating domain

$\mathscr{E}(\phi_2) = 2\pi E(\phi_2/2\pi)$ ($E(x)$ is the integer part of $x$) in the trapped domain and the following functions are defined for each set of $\mu$, $H$, $\bar{\Psi}$ as

$$\begin{aligned} K(\phi_2) &= \frac{\mathscr{E}(\phi_2) + \hat{\theta}(\phi_2) + \delta}{d} \\ h(\phi_2) &= e_s[U(K(\phi_2)) - v_\parallel(\phi_2)\, A(K(\phi_2))] \\ \mathbf{K}(\phi_2) &= K(\phi_2)\, \nabla\Psi + l_0 \nabla\theta + m\nabla\varphi \\ a(\phi_2) &= \left| \frac{\mathbf{B}}{B} \mathbf{x} \mathbf{K}(\phi_2) \right| \left( \frac{2\mu B}{m_s \omega_{cs}^2} \right)^{1/2} \end{aligned} \tag{33}$$

at

$$\theta = \mathscr{E}(\phi_2) + \hat{\theta}(\phi_2)$$
$$\Lambda(\phi_2) = K(\phi_2)\, \hat{\Psi}(\phi_2) + m\hat{\varphi}(\phi_2).$$

The quantity $h_{0,n_2}(\mu, H, \bar{\Psi})$ mainly depends on $\bar{\Psi}$ through the exponential dependence on $(\bar{\Psi} - \Psi_{l_0})/d$ and the functions $v_\parallel(\phi_2)$, $\hat{\theta}(\phi_2)$, $a(\phi_2)$, $\Lambda(\phi_2)$ may be calculated at $\bar{\Psi} = \Psi_{l_0}$. In the circulating domain, the values of $|h_{0,n_2}|^2$ are significant at $\bar{\Psi} = \Psi_{l_0}$ for a set of $n_2 = l_0, l_0 \pm 1, \ldots$, shifted by 1 for a displacement $d$ in $\bar{\Psi}$. In the trapped domain, $\mathscr{E}(\phi_2) = 2\pi E(\phi_2/2\pi)$, the relevant $n_2$ are $0, +1, \ldots$, and $|h_{0,n_2}|^2$ is $d$-periodic in $\bar{\Psi}$. One may note the useful relation

$$\omega_2 \frac{\partial \Lambda}{\partial \phi_2} = \mathbf{K}(\phi_2) \cdot \mathbf{v}_g - m\omega_d. \tag{34}$$

Using the relation

$$d_3\mathbf{x}\, d_3\mathbf{p} = (2\pi)^3\, m_s \frac{dH\, d\mu\, d\bar{\Psi}}{|\omega_2|}, \tag{35}$$

where the transformation (35) must be summed over the two possible signs of $\omega_2$

for circulating particles, the integration over $\bar{\Psi}$ in Eq. (18) after substitution of (29) may be performed over a cell $[0, |d|]$. Note that the first integral in (10) becomes

$$\frac{n_s e_s^2}{T_s} \int_{-\infty}^{+\infty} \frac{2\pi\, d\theta}{|d|} J(\theta)\, B(\theta)\, U(K(\theta))\, U^*(K(\theta)) \tag{36}$$

with

$$K(\theta) = \frac{\theta + \delta}{d}$$

and a similar form may be found for the first integral in (9).

The expression of $\mathscr{L}_{sres}$ is

$$\begin{aligned}\mathscr{L}_{sres} = &-\sum_{n_2} \iint \frac{(2\pi)^3 m_s\, dH\, d\mu}{|\omega_2|\, d^2} \int_0^{|d|} d\bar{\Psi} \frac{F_s}{T_s} \frac{\omega - \omega_s^*}{\omega - n_2\omega_2 - m\omega_3 + i\varepsilon} \\ &\times \iint_{-\infty}^{+\infty} \frac{d\phi_2}{2\pi} \frac{d\phi'}{2\pi} J_0(a(\phi_2))\, h(\phi_2)\, J_0(a(\phi_2'))\, h^*(\phi_2') \\ &\times \exp\left\{ i \left( \Lambda(\phi_2) - \Lambda(\phi_2') + \left( l_0 + \frac{\bar{\Psi} - \Psi_{l_0}}{d} \right) (\mathscr{E}(\phi_2) - \mathscr{E}(\phi_2')) - n_2(\phi_2 - \phi_2') \right) \right\}.\end{aligned} \tag{37}$$

Of course, the integration over $H$ must be performed for the two possible signs of $v_\parallel$ for circulating particles.

For the trapped particle contribution, the bounce and precession frequencies $\omega_2$ and $\omega_3$ do not depend on $\bar{\Psi}$. The integration over $\bar{\Psi}$ then imposes that $\mathscr{E}(\phi_2) = \mathscr{E}(\phi_2')$ and the double integral in the plane $\phi_2$, $\phi_2'$ reduces to cells $2\pi \times 2\pi$ along the diagonal $\phi_2 = \phi_2'$, i.e.,

$$\begin{aligned}\mathscr{L}_{sres} = &-\sum_{n_2} \iint_{\text{trap.}} \frac{(2\pi)^3 m_s\, dH\, d\mu}{|\omega_2\, d|} \frac{F_s}{T_s} \frac{\omega - \omega_s^*}{\omega - n_2\omega_2 - m\omega_3 + i\varepsilon} \\ &\times \sum_p \int_{2p\pi}^{2(p+1)\pi} \frac{d\phi_2}{2\pi} \int_{2p\pi}^{2(p+1)\pi} \frac{d\phi_2'}{2\pi} J_0(a(\phi_2))\, h(\phi_2) \\ &\times J_0(a(\phi_2'))\, h^*(\phi_2') \exp\{ i(\Lambda(\phi_2) - \Lambda(\phi_2') - n_2(\phi_2 - \phi_2')) \}.\end{aligned} \tag{38}$$

Considering only the term $n_2 = 0$, $p = 0$ and assuming $\Lambda = 0$—which is a crude approximation—the trapped ion response obtained by J. Weiland and L. Chen [7] is recovered. On the contrary, for circulating particles, the quantities $n_2\omega_2 + m\omega_3$ depend on $\bar{\Psi}$ through the magnetic shear: $n_2\omega_2 + m\omega_3 = (n_2 + mq(\bar{\Psi}))\ \omega_2 + \omega_d$. Alternative forms of the functionals $\mathscr{L}_{sres}$ more convenient for computations are derived in the next section.

III.3. *Alternative Expression of* $\mathscr{L}_{sres}$

It is useful to transform the resonant terms in (37) by using the relation

$$\frac{1}{\omega - n_2\omega_2 - m\omega_3 + i\varepsilon} = -i\int_0^{+\infty} d\sigma \exp\{i(\omega - n_2\omega_2 - m\omega_3)\,\sigma\} \tag{39}$$

and summing over the indices $n_2$,

$$\begin{aligned}\mathscr{L}_{sres} = i\iint \frac{(2\pi)^3 m_s\, dH\, d\mu}{|\omega_2|\, d^2} \int_0^{|d|} d\bar{\Psi}\, \frac{F_s}{T_s}\, \frac{\omega - \omega_s^*}{|\omega_2|} \\ \times \iint_{-\infty}^{+\infty} \frac{d\phi_2}{2\pi}\, \frac{d\phi_2'}{2\pi}\, \Xi(\phi_2' - \phi_2)\, J_0(a(\phi_2))\, h(\phi_2)\, J_0(a(\phi_2'))\, h^*(\phi_2') \\ \times \exp\left\{ i\left( \frac{\omega - m\omega_3}{\omega_2}(\phi_2' - \phi_2) + \Lambda(\phi_2) - \Lambda(\phi_2') \right.\right. \\ \left.\left. + \left( \frac{\bar{\Psi} - \Psi_{l_0}}{d} + l_0 \right)(\mathscr{E}(\phi_2) - \mathscr{E}(\phi_2')) \right) \right\}\end{aligned} \tag{40}$$

with

$$\Xi(\phi_2' - \phi_2) = \sum_{p=-\infty}^{+\infty} \delta\left( \frac{\phi_2' - \phi_2 + 2p\pi}{\omega_2} - \frac{\omega - m\omega_3}{\omega_2} \right) \tag{41}$$

and $Y$ is the Heaviside function. These expressions can be explicitly given for both types of trajectories.

(i) *Circulating particles.* Since

$$\frac{\omega - m\omega_3}{\omega_2} = \frac{\omega - m\omega_d}{\omega_2} + l_0 + \frac{\bar{\Psi} - \Psi_{l_0}}{d}, \tag{42}$$

the integration over $\bar{\Psi}$ imposes that only the term $p = 0$ remains in (40), (41), and

$$\begin{aligned}\mathscr{L}_{sres} = i\iint_{\text{circ}} \frac{(2\pi)^3 m_s\, dH\, d\mu}{|\omega_2|}\, \frac{F_s}{T_s}\, \frac{\omega - \omega_s^*}{|\omega_2 d|} \\ \times \iint_{-\infty}^{+\infty} \frac{d\phi_2\, d\phi_2'}{2\pi} J_0(a(\phi_2))\, h(\phi_2)\, J_0(a(\phi_2'))\, h^*(\phi_2') \\ \times Y\left( \frac{\phi_2' - \phi_2}{\omega_2} \right) \exp\left\{ i\left( \frac{\omega - m\omega_d}{\omega_2}(\phi_2' - \phi_2) + \Lambda(\phi_2) - \Lambda(\phi_2') \right) \right\}.\end{aligned} \tag{43}$$

For a cylindrical equilibrium and $H \gg \mu B$, the expression calculated by F. Romanelli [6] within the frame of a ballooning electrostatic ($\tilde{A} = 0$) formalism

is easily recovered from (43). The effect of the transverse guiding center motion appears through the function

$$\Lambda'(\phi_2) = \Lambda(\phi_2) + m\frac{\omega_d}{\omega_2}\phi_2 \tag{44}$$

which in view of (34) verifies

$$\omega_2 \frac{\partial \Lambda'}{\partial \phi_2} = \mathbf{K}(\phi_2)\cdot \mathbf{v}_{\mathbf{g}}. \tag{45}$$

(ii) *Trapped particles.* We now have $\omega_3 = \omega_d$ and the integration over $\bar{\Psi}$ in (40) imposes that $E(\phi_2/2\pi) = E(\phi_2'/2\pi)$. We finally obtain

$$\begin{aligned}\mathscr{L}_{sres} = i \iint_{\text{trapped}} & \frac{(2\pi)^3 m_s dH\, d\mu}{|\omega_2|}\frac{F_s}{T_s}\frac{\omega-\omega_s^*}{|\omega_2 d|} \\ & \times \iint_{-\infty}^{+\infty} \frac{d\phi_2\, d\phi_2'}{2\pi} J_0(a(\phi_2))\, h(\phi_2)\, J_0(a(\phi_2'))\, h^*(\phi_2') \\ & \times \delta\left\{E\left(\frac{\phi_2}{2\pi}\right) - E\left(\frac{\phi_2'}{2\pi}\right)\right\} \exp\left\{i\left(\frac{\omega - m\omega_3}{\omega_3}(\phi_2'-\phi_2) + \Lambda(\phi_2) - \Lambda(\phi_2')\right)\right\} \\ & \times \left\{Y\left(\frac{\phi_2'-\phi_2}{\omega_2}\right) + 1 \Big/ \left(\exp\left\{-2i\pi\frac{\omega-m\omega_3}{|\omega_2|}\right\} - 1\right)\right\}.\end{aligned} \tag{46}$$

Again, the transverse guiding center motion is introduced by the function $\Lambda'(\phi_2) = \Lambda(\phi_2) + m(\omega_d/\omega_2)\,\phi_2$ verifying (45). The formula (46) is similar to (43) except the term $1/(\exp\{-2i\pi(\omega - m\omega_3/|\omega_2|)\} - 1)$—resulting from a geometric sum of phase components $\exp 2ip\pi((\omega - m\omega_3)/\omega_2)$ in the $\Xi$ distribution resonant when $\omega = m\omega_3 + n\omega_2$; $n = 0, \pm 1, \pm 2, \ldots$. The formula (46) is consistent with the current and charge responses given by G. Rewoldt, W. M. Tang, and M. S. Chance [8]. However, the resonant form (38), which results directly from our basic frame (18), is only partially recovered in their work. It appears that this form is much more suitable for numerical computations, since the rapid oscillations of the integrand in (46) when $H$ approaches zero ($\omega_2$ behaves like $H$) are avoided when one uses the expression (38).

## IV. WKB Approach

The situation described in Section III corresponds to an infinite sequence of identical structures $U_l(\Psi - \Psi_l)$, $A_l(\Psi - \Psi_l)$ localized on successive resonant surfaces $\Psi = \Psi_l$. In the realistic case of a radially inhomogeneous equilibrium, the

functionals $\mathscr{L}_{l,l'}$ which appear in Eq. (24) depend slowly on $l$ for given $l-l'$. The operators

$$\mathscr{K}_{l,l'} = \frac{\partial \mathscr{L}_{l,l'}}{\partial (U_l^*, A_l^*)}$$

which link a structure

$$U_l(\Psi - \Psi_l),\ A_l(\Psi - \Psi_l)$$

to the neighbouring $U_{l\pm1}(\Psi - \Psi_{l\pm1})$, $A_{l\pm1}(\Psi - \Psi_{l\pm1})$, ..., vary also slowly with $l$. One may then expect that the characteristics of the functions $U_l(X)$, $A_l(X)$ experience a WKB type variation in $l$,

$$(U_l(\Psi - \Psi_l),\ A_l(\Psi - \Psi_l)) = \lambda_l(\bar{U}_l(\Psi - \Psi_1),\ \bar{A}_l(\Psi - \Psi_l)) \exp(i S_l), \tag{47}$$

where the amplitudes $\lambda_l$, the normalized functions $\bar{U}_l(\Psi - \Psi_l)$, $\bar{A}_l(\Psi - \Psi_l)$ and the phase derivatives $\delta_l = \partial S_l / \partial l$ vary slowly with $l$. We may assume $\lambda_l$ and $\delta_l$ real. In fact, Eq. (47) is applicable at all orders in $1/(D\delta \cdot \Delta l)$, where $D\delta$ is the smallest gap between the possible $\delta_l$ solutions and $\Delta l$ is the scale of variation in $l$ of the functionals $\mathscr{L}_{l,l'}$ or operators $\mathscr{K}_{l,l'}$ for given $l-l'$. The condition $1/(D\delta \cdot \Delta l) \ll 1$ is the traditional requirement that the WKB solutions are not coupled through equilibrium inhomogeneity effects.

We may obtain an approximation of $\lambda_l$, $\delta_l$ and $\bar{U}_l(\Psi - \Psi_l)$, $\bar{A}_l(\Psi - \Psi_l)$ by substituting (47) in the functional, freezing the characteristics of the equilibrium at their values on the resonant surface $\Psi_l$. This is exactly what has been done in Section III and the expressions (37) or (43), (46), changing $l_0$ in $l$ and $U$, $A$ in $\bar{U}_l$, $\bar{A}_l$ provide the value $L_l$ of per unit cell $[\Psi_l, \Psi_{l+1}]$,

$$\mathscr{L} = \sum_l |\lambda_l|^2 L_l(\delta_l, \bar{U}_l^*, \bar{A}_1^*, \bar{U}_l, \bar{A}_l). \tag{48}$$

Extremalization of a given $L_l$ with respect to $\bar{U}_l^*$, $\bar{A}_l^*$ produces approximate profiles $\bar{U}_l$, $\bar{A}_l$, and $\delta_l$ eigenvalues, as discussed in Section V. On the other hand, one may derive from the functional $L_l$ interesting informations on the whole mode $\tilde{U}$, $\tilde{A}$. We recall that, for a real frequency $\omega$, the power which is transferred from the mode to the particles is $2\omega\ \mathrm{Im}(\mathscr{L})$, i.e., $2\omega \lambda_l^2\ \mathrm{Im}(L_l)$ per cell $[\Psi_l, \Psi_{l+1}]$. We will assume that $\mathrm{Im}(L_l)$ is a perturbation in $L_l$, so that we may write, for real $\delta_l$,

$$\mathscr{L} = \sum_l \left\{ \mathrm{Re}\left( L_l |\lambda_l|^2 + \frac{1}{i} \frac{\partial L_l}{\partial \delta_l} \frac{\partial \lambda_l}{\partial l} \lambda_l^* \right) + i |\lambda_l|^2\ \mathrm{Im}(L_l) \right\}, \tag{49}$$

where $\partial L_l / \partial \delta_l$ may be replaced by $\partial\ \mathrm{Re}(L_l)/\partial \delta_l$. Extremalization with respect to $\lambda_l^*$ then provides

$$\mathrm{Re}(L_l)\ \lambda_l + \frac{1}{2i} \left\{ \frac{\partial\ \mathrm{Re}(L_l)}{\partial \delta_l} \frac{\partial \lambda_l}{\partial l} + \frac{\partial}{\partial l} \left( \lambda_l \frac{\partial\ \mathrm{Re}(L_l)}{\partial \delta_l} \right) \right\} + i \lambda_l\ \mathrm{Im}(L_l) = 0; \tag{50}$$

i.e., the WKB relations giving $\delta_l$ (real) and the variations of the real amplitudes $\lambda_l$ are

$$\begin{aligned} &\mathrm{Re}(L_l(\delta_l, \bar{U}_l^*, \bar{A}_l^*, \bar{U}_l, \bar{A}_l)) = 0 \\ &\frac{\partial}{\partial l}\left(\frac{\partial\, \mathrm{Re}(L_l)}{\partial \delta_l}\lambda_l^2\right) = 2\lambda_l^2\, \mathrm{Im}(L_l). \end{aligned} \tag{51}$$

This last equation can be considered as a balance equation between the energy $2\omega\,\lambda_l^2\,\mathrm{Im}(L_l)$ transferred from the mode to the particles per cell $[\Psi_l, \Psi_{l+1}]$ and the energy flux $-\omega(\partial(\mathrm{Re}(L_l))/\partial\delta_l)\,\lambda_l^2$ (averaged in each cell) carried by the mode $\tilde{U}$, $\tilde{A}$ across the magnetic surfaces. There exists also a similar flux of momentum around the major axis in the ratio of the toroidal wave number $m$ to the frequency $\omega$. Generally, the quantity $2m\,\mathrm{Im}(L_l)$ represents the momentum transferred per unit time from the mode to the particles in the cell $[\Psi_l, \Psi_{l+1}]$. By expressing the balance between that force and the Lorentz force associated with the quasilinear flux of particles, the latter (for a given species at a given energy $H$) may be directly derived from the expressions of $L_l$.

## V. Numerical Computations

### V.1. *Discretisation*

We have implemented in the code TORRID the exact expressions of the functional $\mathscr{L}(U^*(K), A^*(K), U(K), A(K))$ per cell $[\Psi_l, \Psi_{l+1}]$ given by the formula (37) or (43), (46). That formula may be formally written

$$\mathscr{L} = \iint dK\, dK'\, (U^*(K), A^*(K))\, N(K, K')(U(K'), A(K')), \tag{52}$$

where $N(K, K')$ is a complex kernel depending analytically on the frequency $\omega$ and the phase shift $\delta$. The expression (52) is valid only if the functions $U(\Psi - \Psi_l)$, $A(\Psi - \Psi_l)$ are localized in $\Psi - \Psi_l$. This may be checked by a preliminary spatial WKB analysis $U(\Psi - \Psi_l)$, $A(\Psi - \Psi_l) \sim \exp\{i(K_\Psi(\Psi - \Psi_l))\}$ for large $|\Psi - \Psi_l|$, ensuring that no solution with real $K_\Psi$ exists. Then the Fourier functions $U(K)$, $A(K)$ of $U(\Psi - \Psi_l)$, $A(\Psi - \Psi_l)$ have no singularities in $K$. From the computational point of view, this allows to develop those functions over a set of squared integrable functions $P_n(K)$. Zero order finite elements appear suitable to insure both numerical stability and proper accuracy. We write

$$(U(K), A(K)) = \sum_{n=-N}^{N} a_n P_n(K), \tag{53}$$

where the $P_n(K)$ are window functions in successive small intervals $\alpha$ over an interval $(-\Delta K, \Delta K)$. The quantities $1/\alpha$ and $1/\Delta K$ reflect of course the largest and

smallest scale in $\Psi$ of the functions $U(\Psi - \Psi_l)$, $A(\Psi - \Psi_l)$. The ratio $N = \Delta K/\alpha$ is typically of order 100. Substitution of (53) in (52) yields the expression

$$\mathscr{L} = \sum_{m,n} a_m^* L_{mn} a_n \tag{54}$$

$$L_{mn} = \iint dK\, dK'\, P_m(K)\, N(K, K')\, P_n(K'). \tag{55}$$

Expressing that the functional (54) is extremum with respect to the $a_m^*$ leads to the set of linear equations

$$\sum_{n=-N}^{N} L_{mn} a_n = 0. \tag{56}$$

Note that $a_n$ reflects the 2 components $U$, $A$ at given $K = n\alpha$, so that $[2(2N+1)]^2$ matrix elements are actually involved in (56). For given equilibrium and $\omega$, $m$, $l_0$, $\delta$, the eigenmodes $U$, $A$ are derived by expressing the degeneracy of the matrix $L_{mn}$. A first numerical problem is the computation of the matrix elements with the proper accuracy. A second problem is the investigation of the degeneracy of the matrix $L_{mn}$ when varying the plasma and mode parameters.

V.2. *Matrix Elements Computation and Investigation of Eigenmodes*

Each matrix element is a 4-$d$ integral over $\phi_2$, $\phi_2'$ within intervals of small amplitude proportional to the window thickness $\alpha$, and over the constants of motion $H$, $\mu$ within the circulating and trapped domains.

The main difficulty is that the integrand in $H$, $\mu$ plane at a given ratio $H/\mu$ exhibits strongly oscillating features. While analytical integration is possible in special cases (ultra circulating $H \gg \mu B$) or trapped ($H \sim \mu B$) particles, the use of standard varying meshes methods is unavoidable to cover the general case. The computational time on Cray X-MP is then typically 500 s for a whole matrix $L_{mn}$, [illegible] matrix computation.

Computational time can be saved in a general investigation of eigenmodes by exploiting the fact that the matrix $L_{mn}$ depends linearly on some parameters of equilibrium such as the average density, the density and temperature gradients.

Being $\lambda_1$ and $\lambda_2$ two such parameters, $L_{mn}$ may be written

$$L_{mn} = L_{mn}^{(0)} + \lambda_1 L_{mn}^{(1)} + \lambda_2 L_{mn}^{(2)}. \tag{57}$$

The three matrixes $L_{mn}^{(0)}$, $L_{mn}^{(1)}$, and $L_{mn}^{(2)}$ allow a fast computation of the matrix $L_{mn}$ in the plane $(\lambda_1, \lambda_2)$. The determination of critical $(\lambda_1, \lambda_2)$ and the corresponding $U$, $A$ may then be performed. The numerical method is a standard Gauss routine which transforms the matrix $L$ in a product $T.U$ of triangular matrixes, the diagonal of $U$ containing the successive maximal pivots. The last pivot $\pi(\lambda_1, \lambda_2)$

reflects the smallest eigenvalue of the matrix $L_{mn}$ and cancels at degenerate points $(\lambda_1, \lambda_2)$. The corresponding eigenmode $U$, $A$ may be derived by solving the triangular system

$$\sum_m U_{mn} a_n = 0.$$

The process for finding $(\lambda_1, \lambda_2)$ includes two steps: first building a map of the modulus $|\pi(\lambda_1, \lambda_2)|$ over a $(\lambda_1, \lambda_2)$ grid, and then applying an iterative Newton–Raphson method near each significant dip. The two situations of a set of isolated degeneracy points $(\lambda_1, \lambda_2)$ or of continuum along a curve are encountered. In the latter case, a Newton method where $\mathrm{Re}(\pi(\lambda_1, \lambda_2))$ and $\mathrm{Im}(\pi(\lambda_1, \lambda_2))$ are replaced by their tangent values does not converge. A one-dimensional Newton method must then be used.

V.3. *Example of Application*

As an example, we show an investigation of the effect of coupling between harmonics $l$, $l'$ for electrostatic modes driven unstable by the diamagnetism of circulating ions. We consider first a cylindrical equilibrium of concentric magnetic surfaces (which may then be labelled by their minor radius $r$, rather than by their poloidal flux $\Psi$, $d\Psi = -B_\theta R\, dr$) and have consequently $\mathscr{L}_{ll'} = 0$ for $l \neq l'$. The electron response is assumed to be adiabatic and the equation $\partial \mathscr{L}_{l,l}/\partial U^* = 0$ (Eqs. (10) and (18)) yields the usual equation for the electric potential structure $U(\Psi - \Psi_l)$,

$$\left\{2 - \left\langle J_0(K_\perp \rho_{ci}) \cdot \frac{\omega - \omega_i^*}{\omega - K_\parallel v_\parallel + i\varepsilon} J_0(K_\perp \rho_{ci}) \cdot \right\rangle\right\} U(\Psi - \Psi_l) = 0, \tag{58}$$

where $K_\parallel = (1/R)(m + l/q(\Psi))$ is the parallel wave vector, the bracket indicates a Maxwellian average over parallel and perpendicular velocities $v_\parallel$ and $v_\perp$, and $J_0$. is a Bessel operator with

$$K_\perp \rho_{ci} = \left\{\left(-i\frac{\partial}{\partial r}\right)^2 + \frac{l^2}{r^2}\right\}^{1/2} \frac{m_i v_\perp}{e_i B}.$$

Removing the ion Larmor radius effects by putting $\rho_{ci} = 0$, a very simple case appears: Eq. (58) then imposes that $U$ is localized at a $\Psi$ value such that

$$\left(\frac{\Psi - \Psi_l}{\delta_i}\right)^2 = \frac{\omega_{Ti}^*}{2\omega} \tag{59}$$

with

$$\omega = \frac{\omega_{Ti}^*}{2} - \omega_{ni}^* \tag{60}$$

and $\delta_i = (qR\omega/v_i)\, d$, $v_i = \sqrt{2T_i/m_i}$. This situation allows us to test the ability of the code to reproduce complex structures $U(\Psi - \Psi_l)$, through the system of Eqs. (56) acting on Fourier components $U(K)$. The computed radial profiles are effectively localized around the $\Psi$ value given by (59) within the expected width $\sim 1/N$ determined by the number $N$ of window functions. The considered case exhibits a degeneracy in the plane $\lambda_1 = \omega_{ni}^*/\omega$, $\lambda_2 = \omega_{Ti}^*/\omega$, since all the solutions lie along the line derived from (60).

Taking now into account finite Larmor radius effects ($\rho_{ci} \neq 0$), Eq. (58) produces ionic modes in cylindrical geometry for given normalized parameters $\delta_i$ and $(l/r)\,\rho_i (\rho_i = m_i v_i / e_i B_0)$ by scanning over $\lambda_1 = \omega_{ni}^*/\omega$, $\lambda_2 = \omega_{Ti}^*/\omega$. For $\mathrm{Im}(\omega)$ of order of $\mathrm{Re}(\omega)$, the profiles we obtain (Fig. 1) fit well the nearly gaussian shape already found by R. E. Waltz, W. Pfeiffer, and D. Dominguez [9]. Marginal ($\mathrm{Im}(\omega) = 0$) radial structures for relatively low values of $\eta_i = \lambda_2/\lambda_1$ are shown on Fig. 2. The mode then essentially consists of two propagative waves, symmetric with respect to the surface $\Psi = \Psi_l$, each of those waves carrying energy from a region (A), where it gains energy (negative contribution to $2\omega\ \mathrm{Im}(\mathscr{L})$), to a region (B), where it returns energy (positive contribution to $2\omega\ \mathrm{Im}(\mathscr{L})$). The computed structure in the central region between (A) and (B) is consistent with a WKB approach based on Eq. (58). The instability is limited by the fact that the variation of the dispersive properties of the plasma must ensure enough reflection on both ends of the wave domain of existence. Figure 3 shows the amplitude of the propagative component $U_+$ and the reflected past $U_-$.

Finally we consider the same type of convective mode in a realistic noncylindrical

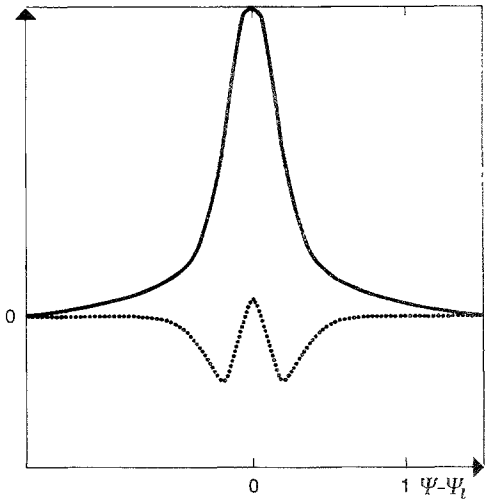


FIG. 1. Radial profile $U(\Psi - \Psi_1)$ of an unstable $\eta_i$ mode in a cylindrical geometry (the solid and the dashed lines represent the real and imaginary parts of $U$): $\delta_i = 0.88(d\Psi/dr)\ \rho_i$, $(l/r)\,\rho_i = 1$, $T_e/T_i = 2$, $\mathrm{Im}(\omega)/\mathrm{Re}(\omega) = 0.95$, $\omega_{ni}^*/\omega = 11.36$, $\omega_{Ti}^*/\omega = 25.76$, the $\Psi$ unit is 5 $(d\Psi/dr)\ \rho_i$, and $N = 70$.

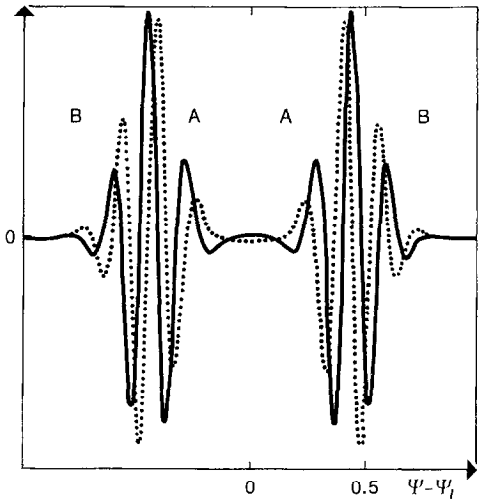


FIG. 2. Radial profile $U(\Psi-\Psi_l)$ of a marginal $\eta_i$ mode in a cylindrical geometry. Energy is convected from region A to region B: $\delta_i = 2\,(d\Psi/dr)\,\rho_i$, $(l/r)\,\rho_i = 0.1$, $T_e/T_i = 1$, $\omega^*_{ni}/\omega = 13.8$, $\omega^*_{Ti}/\omega = 45.5$, the $\Psi$ unit is 4 $(d\Psi/dr)\,\rho_i$, and $N = 70$.

geometry. Due to the coupling between poloidal harmonics $l$, $l'$, the harmonic $l$ may drive energy from the harmonic $l-1, \ldots$, and transfer energy to the component $l+1, \ldots$. This effect is expected to replace the reflection mechanism in the pure cylindrical case, for achieving the mode consistency. Figure 4 shows a computed profile which is purely propagative and corresponds to a large overlapping of harmonics.

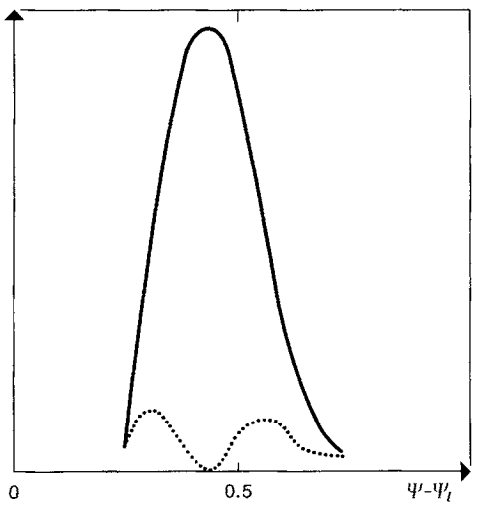


FIG. 3. Amplitudes of the component $U_+$ propagating away from the resonant surface $\Psi = \Psi_l$ (solid line) and the reflected part $U_-$ (dashed line). Same mode as on Fig. 2.

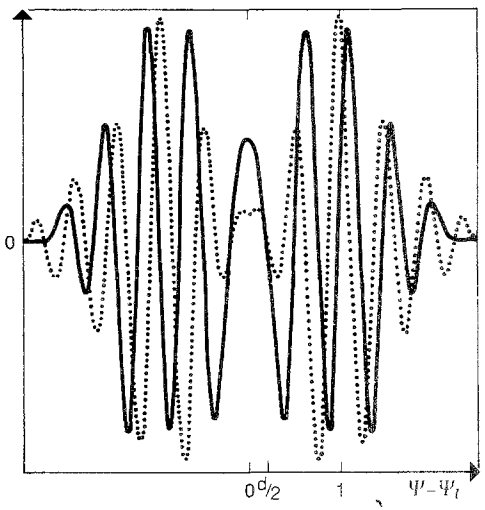


FIG. 4. Standard radial profile $U(\Psi - \Psi_l)$ of a marginal $\eta_i$ mode about $\Psi = \Psi_l$ in a toroidal geometry: $q(\Psi_l) = 2$, $d = \delta_l = 2(d\Psi/dr)\ \rho_i$, $(l/r)\ \rho_i = 0.1$, $T_e/T_i = 1$, $\omega^*_{ni}/\omega = 13.8$, $\omega^*_{Ti}/\omega = 27$. Same scale as on Fig. 2 ($N = 70$), the threshold $\eta_i$ is smaller by a factor 1.7.

For $N \leqslant 100$, the code actually needs a 900,000 word memory size on a CRAY X-MP and the storage of the three symmetric complex matrixes $L^{(0)}$, $L^{(1)}$, $L^{(2)}$ requires 6 $(2N+1)(4N+3)$ words. The CPU matrix computation time is less than 500 s. The inversion time is 0.4 s for $N = 70$ and about 100 inversions are necessary to find an eigenmode in a plane $\lambda_1$, $\lambda_2$. Consequently, for given $l, m, \omega, \delta$ and magnetic geometry, the code provides routinely two equilibrium parameters $\lambda_1 = (1/n_i)(\partial n_i/\partial \Psi)$ and $\lambda_2 = (1/T_i)(\partial T_i/\partial \Psi)$ within 600 s CPU.

## CONCLUSION

In order to investigate electromagnetic microinstabilities in tokamaks, a numerically tractable variational method, exploiting integrability of the trajectories of charged particles in the equilibrium magnetic field, has been established and described in detail in this work. The coupling of poloidal harmonics due to the toroidal effects is included within the frame of a ballooning formalism which appears as the lowest order of a WKB analysis with respect to the poloidal wave numbers. The formalism allows us to implement the exact circulating and trapped particle response to the turbulent field in the actual tokamak geometry. Circulating and trapped particle contributions to the variational functional are written under various forms to facilitate numerical computations. The numerical code TORRID exploiting those expressions has been built and checked successfully. It should be a convenient tool for systematic studies of the linear instabilities in tokamaks and

the associated quasilinear transport mechanisms. As an example, we have shown that the curvature effects lower the threshold $\eta_i = d \operatorname{Log} T_i / d \operatorname{Log} n_i$ and delocalize the radial profiles of ionic modes.

## APPENDIX I

In the usual ballooning representation [3], an eigenfunction $f$ is looked for as a $\theta$-periodization of

$$\hat{f}(\Psi, \theta) = A(\theta) \exp\{im(\varphi - q(\Psi)\,\theta)\},$$

where $A$ is a slowly varying function of $\theta$. The function $f$ can be developed in Fourier series of $\theta$,

$$f(\Psi, \theta) = \sum_l f_l(\Psi) \exp(il\theta),$$

where the $f_l$ components are the Fourier transforms of the nonperiodic function $\hat{f}$ for integer values,

$$f_l(\Psi) = \int_{-\infty}^{+\infty} \frac{d\theta}{2\pi} A(\theta) \exp\{i(m(\varphi - q(\Psi)\,\theta) - l\theta)\}.$$

Using $mq(\Psi) = -l_0 - (\Psi - \Psi_{l_0})/d$ and the Fourier transform $\bar{A}(s)$ of $A(\theta)$, $f_l$ is changed in

$$f_l(\Psi) = \int_{-\infty}^{+\infty} \frac{d\theta}{2\pi}\, ds\, \bar{A}(s) \exp\left\{i\left(\left[-s + l_0 + \frac{\Psi - \Psi_{l_0}}{d} - l\right]\theta + m\varphi\right)\right\}$$

$$f_l(\Psi) = \bar{A}\left(\frac{\Psi - \Psi_l}{d}\right)$$

and, finally,

$$f(\Psi, \theta) = \sum_l \bar{A}\left(\frac{\Psi - \Psi_l}{d}\right) \exp\{i\,(l\theta + m\varphi)\}$$

which is equivalent to (7) and (27) with $\delta = 0$.

## REFERENCES

1. A. SAMAIN, in *Proceedings, 4th Europ. Conf. on Controlled Fusion and Plasma Physics, Rome*, 1970, Vol. 1, p. 145.

2. J. B. TAYLOR, in *Plasma Physics and Controlled Nuclear Fusion Research* (IAEA, Vienna, 1977), Vol. 2, p. 323.
3. J. W. CONNOR, R. J. HASTIE, AND J. B. TAYLOR, *Proc. Roy. Soc. London A* **365**, 1 (1979).
4. A. SAMAIN, *Nucl. Fusion* **10**, 325 (1970).
5. J. R. HASTIE AND J. B. TAYLOR, *Plasma Phys.* **10**, 479 (1968).
6. F. ROMANELLI, *JET Rep. JET P* 07 (1988).
7. J. WEILAND AND L. CHEN, *Phys. Fluids* **28**, 1359 (1985).
8. G. REWOLDT, W. M. TANG, AND M. S. CHANCE, *Phys. Fluids* **25**, 480 (1982).
9. R. E. WALTZ, W. PFEIFFER, AND R. R. DOMINGUEZ, *Nucl. Fusion* **20**, 43 (1980).